

## LONG-RANGE AND SHORT-RANGE ORDER IN GEM PARGASITE FROM MYANMAR: CRYSTAL-STRUCTURE REFINEMENT AND INFRARED SPECTROSCOPY

DAVID HEAVEYSEGE, YASSIR A. ABDU, AND FRANK C. HAWTHORNE<sup>§</sup>

*Department of Geological Sciences, University of Manitoba, 125 Dysart Road, Winnipeg, Manitoba R3T 2N2, Canada*

### ABSTRACT

The crystal structure of pargasite from a cut gem from Myanmar,  $(K_{0.094}Na_{0.93})(Na_{0.15}Ca_{1.78})(Mg_{4.51}Fe^{2+}_{0.02}Al_{0.53}Ti_{0.10})(Si_{6.56}Al_{1.44})O_{22}(OH_{1.32}F_{0.68})$ ,  $a$  9.882(6),  $b$  17.973(11),  $c$  5.282(3) Å,  $\beta$  105.20(1)°,  $V$  905.33(17) Å<sup>3</sup>, space group  $C2/m$ ,  $Z = 2$ , has been refined to an  $R_1$  index of 1.9% using  $MoK\alpha$  single-crystal X-ray diffraction. The unit formula (calculated from the results of electron-microprobe analysis), the refined site-scattering values, and the observed mean bond-lengths, were used to assign site populations. <sup>14</sup>Al occurs at both the  $T(1)$  and  $T(2)$  sites, but is strongly ordered at  $T(1)$ . <sup>61</sup>Al is disordered over the  $M(2)$  and  $M(3)$  sites, but is excluded from the  $M(1)$  site. <sup>23</sup>Na is split between the  $A(2)$  and  $A(m)$  sites with minor K assigned to the  $A(m)$  site. The frequencies of short-range ion arrangements over the configuration symbol  $M(1)M(1)M(3)-O(3)-A:T(1)T(1)$  were calculated from the refined site-populations and are in reasonable accord with the fitted infrared spectrum of this amphibole in the principal OH-stretching region.

**Keywords:** pargasite, amphibole, gem, crystal structure, infrared spectroscopy, Myanmar, short-range order.

### INTRODUCTION

Pargasite is a monoclinic calcium amphibole with the  $C2/m$  structure and an endmember formula  $NaCa_2Mg_4AlSi_6Al_2O_{22}(OH)_2$  (Hawthorne *et al.* 2012), and both pargasite (*e.g.*, Oberti *et al.* 1995a, Tait *et al.* 2001) and fluoro-pargasite (Lupulescu *et al.* 2005, Della Ventura *et al.* 2014) and their synthetic analogues (Raudsepp *et al.* 1987a, Oberti *et al.* 1995b) have been characterized. The infrared spectra of amphiboles contain significant information concerning the short-range order of cations and anions in the amphibole structure. This information can only rarely be extracted from natural amphiboles as their chemical compositions give rise to many bands in the principal OH-stretching region and the resultant spectra do not contain enough information to fit the spectra correctly. Consequently, most of our knowledge of short-range order comes from work on synthetic amphiboles. However, gem-quality amphiboles are generally of much simpler chemical composition than common amphiboles (particularly because they have very low Fe content), making it more feasible to fit the infrared spectra correctly. During routine identification of gemstone amphiboles, the discovery of a gem with a composition close to pargasite<sub>50</sub>–edenite<sub>50</sub> gave us the

opportunity to characterize the long-range and short-range structure of this amphibole.

### EXPERIMENTAL

The sample is a transparent colorless roval-cut gemstone measuring  $9 \times 10 \times 5$  mm (Fig. 1), and was obtained from a gem dealer. Fragments for experimental work were removed from the girdle of the stone.

#### *X-ray diffraction*

A small fragment of amphibole was selected for X-ray diffraction measurements; the fragment was clear and free from inclusions. The crystal was attached to a tapered glass fiber and mounted on a Bruker D8 three-circle diffractometer equipped with a rotating-anode generator producing monochromatic  $MoK\alpha$  X-radiation, multilayer optics and an APEX-II CCD detector. The intensities of 16,196 reflections were collected to  $\sim 60^\circ 2\theta$  using 15 s per  $0.2^\circ$  frame with a crystal-to-detector distance of 5 cm. Empirical absorption corrections (SADABS, Sheldrick 2008) were applied. The unit-cell parameters were obtained by least-squares refinement from the positions of 1375 reflections with  $I > 10\sigma I$ , and are given in Table 1.

<sup>§</sup> Corresponding author email address: frank\_hawthorne@umanitoba.ca



FIG. 1. View of gem pargasite from Myanmar; the stone is  $9 \times 10$  mm and 4.05 ct, and the small V cut in the girdle is where the material was taken for this work.

The crystal structure was refined with the Bruker SHELXTL Version 5.1 suite of programs (Sheldrick 2008). Scattering curves for neutral atoms were taken from the International Tables for Crystallography (1992). The  $R$  indices are of the form given in Table 1, and are expressed as percentages. The structure was refined to an  $R_1$  index of 1.92%, with anisotropic-displacement parameters for all sites except  $A(2)$  and  $A(m)$ . Atom positions and anisotropic-displacement parameters are given in Table 2, selected interatomic distances in Table 3, and refined site-scattering values (Hawthorne *et al.* 1995) and assigned site-populations in Table 4, and a bond-valence analysis is given in Table 5. A table of structure factors and a cif file are available from the Depository of Unpublished Data on the Mineralogical Association of Canada website (document gem pargasite CM53-3\_10.3749/canmin.1400107).

### Electron Microprobe Analysis (EMPA)

The crystal used for the collection of the X-ray intensity data was subsequently mounted in epoxy, polished, and analyzed with a CAMECA SX-100 electron microprobe operating in wavelength-dispersion mode with the following conditions: excitation voltage, 15 kV; specimen current, 10 nA; beam size, 5  $\mu\text{m}$ ; peak count time, 10 s; background count time, 10 s. The crystal was analyzed at 10 points using the following standards for  $K\alpha$  lines: albite, Na; diopside, Si, Ca; andalusite, Al; riebeckite, F; forsterite, Mg; orthoclase, K; fayalite, Fe; spessartine, Mn; titanite, Ti;  $\text{LaVO}_4$ , V; chromite, Cr; pentlandite, Ni; and gahnite, Zn. Data were corrected using the PAP procedure of Pouchou & Pichoir (1985), and the mean chemical composition is given in Table 6, together with the unit formula calculated on the basis of 24 (O,OH,F,Cl).

### Infrared spectroscopy

The unpolarized FTIR spectrum was collected using a Bruker Tensor 27 FTIR spectrometer equipped with a KBr beam splitter and a DLATGS detector. The spectrum over the range  $4000\text{--}400\text{ cm}^{-1}$  was obtained by averaging 100 scans with a resolution of  $4\text{ cm}^{-1}$ . Baseline correction was done using the OPUS spectroscopic software (Bruker Optic GmbH). The spectrum is shown in Figure 2. At the moment, we do not know how many bands to expect in this spectrum, and consequently we choose to fit an increasing number of peaks to the envelope until we get a fit that encompasses all changes in the first- and second-derivatives of the envelope as a function of wavenumber (Fig. 2).

### SITE POPULATIONS

The  $C2/m$  amphibole structure is shown in Figure 3. Although this is a familiar structure, Figure 3 will be essential in understanding the complexities of short-range arrangements in amphiboles.

TABLE 1. SUMMARY OF CRYSTALLOGRAPHIC, DATA COLLECTION, AND STRUCTURE REFINEMENT INFORMATION FOR GEM PARGASITE

$a$ (Å)	9.882(6)	Crystal size ( $\mu\text{m}$ )	$50 \times 50 \times 100$
$b$ (Å)	17.973(11)	Radiation/monochromometer	MoK $\alpha$
$c$ (Å)	5.282(3)	No. of reflections	16196
$\alpha$ ( $^\circ$ )	90	No. unique reflections	1375
$\beta$ ( $^\circ$ )	105.20(14)	$R_1$ %	1.92
$\gamma$ ( $^\circ$ )	90	$R_{\text{merge}}$ %	1.16
Space group	$C2/m$	wR% <sup>2</sup>	5.03
Z	2	GoF	1.102

Cell content:  $2[(\text{K}_{0.094}\text{Na}_{0.93})(\text{Na}_{0.144}\text{Ca}_{1.781})(\text{Mg}_{4.513}\text{Fe}^{2+}_{0.023}\text{Al}_{0.529}\text{Ti}_{0.10})(\text{Si}_{6.557}\text{Al}_{1.443})\text{O}_{22}(\text{OH},\text{F})_2]$

TABLE 2. ATOM COORDINATES AND DISPLACEMENT PARAMETERS FOR GEM PARGASITE

Site	x	y	z	$U_{11}$	$U_{22}$	$U_{33}$	$U_{23}$	$U_{13}$	$U_{12}$	$U_{eq}$
T(1)	0.28002(3)	0.08509(2)	0.30204(6)	0.00805(17)	0.00820(17)	0.00822(17)	-0.00025(10)	0.00183(12)	-0.00050(10)	0.00821(11)
T(2)	0.28961(3)	0.17279(2)	0.81069(6)	0.00704(17)	0.00742(17)	0.00673(17)	0.00029(10)	0.00204(11)	-0.00039(10)	0.00702(11)
M(1)	0	0.08903(3)	½	0.0079(3)	0.0068(3)	0.0059(3)	0	0.0025(2)	0	0.0067(2)
M(2)	0	0.17625(3)	0	0.0068(3)	0.0061(3)	0.0062(3)	0	0.00236(19)	0	0.00624(19)
M(3)	0	0	0	0.0072(4)	0.0059(4)	0.0057(4)	0	0.0015(3)	0	0.0063(3)
M(4)	0	0.27904(2)	½	0.0133(2)	0.01055(19)	0.01161(19)	0	0.00666(13)	0	0.01117(13)
A(2)	0	0.4702(14)	0	0.026(4)	0.029(9)	0.041(5)	0	0.023(4)	0	0.029(4)
A(m)	0.0309(19)	½	0.068(4)	0.061(6)	0.048(8)	0.078(7)	0	0.059(6)	0	0.055(4)
O(1)	0.10776(9)	0.08625(5)	0.21788(17)	0.0084(4)	0.0135(4)	0.0092(4)	-0.0007(3)	0.002(3)	-0.0017(3)	0.01041(19)
O(2)	0.11942(9)	0.17191(5)	0.72961(17)	0.0067(4)	0.0108(4)	0.0101(4)	0.0008(3)	0.0017(3)	0.0000(3)	0.00929(18)
O(3)	0.10704(12)	0	0.7165(2)	0.0114(6)	0.0122(6)	0.0133(6)	0	0.0030(4)	0	0.0123(4)
O(4)	0.36555(9)	0.24988(5)	0.78862(17)	0.0131(4)	0.0102(4)	0.0127(4)	-0.0002(3)	0.0047(3)	-0.0027(3)	0.01176(19)
O(5)	0.34963(9)	0.13894(6)	0.10968(17)	0.0107(4)	0.0172(5)	0.0100(4)	0.0048(3)	0.0011(3)	-0.0002(3)	0.01296(19)
O(6)	0.34468(9)	0.11558(5)	0.60947(17)	0.0104(4)	0.0147(4)	0.0132(4)	-0.0043(3)	0.0032(3)	0.0009(3)	0.01273(19)
O(7)	0.34177(14)	0	0.2772(3)	0.0118(6)	0.0124(6)	0.0190(6)	0	0.0034(5)	0	0.0145(3)

*The T sites*

The unit formula indicates significant Al at the *T* sites (Table 5) and the ordering of Al over the *T*(1) and *T*(2) sites is of considerable interest. This issue of Al/Si order has been examined by many authors using  $\langle T-O \rangle$  bond-lengths (Papike *et al.* 1969, Hawthorne & Grundy 1973a, b, 1977, Robinson *et al.* 1973, Bocchio *et al.* 1978, Hawthorne 1981, 1983a, b, Oberti *et al.* 1995a). More recently, this issue has been examined using more direct approaches, and the preference of  $^{[4]}\text{Al}$  for *T*(1) has been confirmed by neutron diffraction (Welch & Knight 1999) and spectroscopic methods (Welch *et al.* 1994, 1998, Jenkins *et al.* 1997, Gottschalk & Andrut 2003, Najorka & Gottschalk 2003, Della Ventura *et al.* 2007). Hawthorne & Oberti (2007) reviewed previous work on this issue and presented new relations between mean *T-O* bond-lengths and Al site-populations. They showed that the grand  $\langle T-O \rangle$  distance is strongly affected by inductive effects where  $^{[4]}\text{Al}$  is less than 0.50 *apfu*, but varies linearly with  $^{[4]}\text{Al}$  content where  $^{[4]}\text{Al}$  is greater than 0.50 *apfu*. Hawthorne & Oberti (2007) derived the following equation relating grand  $\langle T-O \rangle$  distance to  $^{[4]}\text{Al}$  content:  $\text{grand } \langle T-O \rangle = 1.6250 + 0.0153 ^{[4]}\text{Al}$ , where  $^{[4]}\text{Al} > 0.50$  *apfu*. For the gem pargasite, this equation predicts a grand  $\langle T-O \rangle$  distance of 1.647 Å, in close accord with the observed value of 1.649 Å (Table 3). Hawthorne & Oberti (2007) also presented relations between mean *T-O* bond-lengths and Al site-populations for the *T*(1) and *T*(2) tetrahedra; the site populations calculated from these equations were adjusted slightly (Table 6) so that they show an equally good fit to the equations of Hawthorne & Oberti (2007) and the bulk composition of the crystal given in Table 6.

*The M(1,2,3) sites*

There has been considerable diffraction and spectroscopic work on cation and anion order in this part of the amphibole structure, and detailed discussions of this work are given by Hawthorne (1981, 1983a), Hawthorne & Oberti (2007), Hawthorne & Della Ventura (2007), and Oberti *et al.* (2007). The total refined scattering at the *M*(1,2,3) sites (59.6 *epfu*, Table 4) is in close agreement with the total effective scattering of the C-group cations in the structural formula calculated from the electron-microprobe analysis: 60.6 *epfu* (Table 6), allowing use of the unit formula (Table 6) as a guide for assigning the *M*(1,2,3) site populations. We adjusted the refined site-scattering values slightly such that their sum corresponds to that from the structural formula: *M*(1) 24.1, *M*(2) 24.4, *M*(3) 12.1 *epfu*. The C-group cations to be assigned are 4.47 Mg + 0.53 Al (Table 6). Obviously Mg must dominate at every site; the issue is where does the Al occur. As the X-ray scattering factors of Mg ( $Z = 12$ ) and Al ( $Z = 13$ ) are very close, we must

TABLE 3. SELECTED INTERATOMIC DISTANCES (Å) IN GEM PARGASITE

T(1)–O(1)	1.643(1)	T(2)–O(2)	1.623(1)
T(1)–O(5)	1.675(1)	T(2)–O(4)	1.594(1)
T(1)–O(6)	1.673(1)	T(2)–O(5)	1.650(1)
T(1)–O(7)	1.664(1)	T(2)–O(6)	1.669(1)
<T(1)–O>	1.664	<T(2)–O>	1.634
M(1)–O(1) ×2	2.046(1)	M(2)–O(1) ×2	2.105(1)
M(1)–O(2) ×2	2.081(1)	M(2)–O(2) ×2	2.079(1)
M(1)–O(3)	2.086(1)	M(2)–O(4) ×2	1.999(1)
<M(1)–O>	2.071	<M(2)–O>	2.061
M(3)–O(1) ×4	2.054(1)	M(4)–O(2) ×2	2.412(1)
M(3)–O(3) ×2	2.047(2)	M(4)–O(4) ×2	2.328(1)
<M(3)–O>	2.051	M(4)–O(5) ×2	2.650(1)
A(m)–O(5) ×2	3.015(4)	M(4)–O(6) ×2	2.596(1)
A(m)–O(6) ×2	2.762(14)	<M(4)–O>	2.497
A(m)–O(7)	2.407(8)	A(2)–O(5) ×2	2.616(18)
A(m)–O(7)	2.472(8)	A(2)–O(6) ×2	2.707(13)
<A(m)–O>	2.664	A(2)–O(7) ×2	2.464(56)
		<A(2)–O>	2.596
A(2)–A(m)	0.672(8)		
A(m)–A(m)	0.81(4)		
A(2)–A(2)	1.07(5)		

TABLE 4. REFINED SITE-SCATTERING VALUES, MEAN BOND-LENGTHS, AND ASSIGNED SITE-POPULATIONS FOR GEM PARGASITE

Site	Site scattering* ( <i>epfu</i> )	Site population ( <i>apfu</i> )	Mean bond-length (Å)
T(1)	56	2.46 Si + 1.54 Al	1.664
T(2)	56	4 Si	1.634
M(1)	23.71(9)	1.99 Mg + 0.01 Al	2.071
M(2)	24.04(9)	1.66 Mg + 0.33 Al	2.061
M(3)	11.89(6)	0.86 Mg + 0.14 Al	2.051
M(4)	37.96(9)	1.78 Ca + 0.22 Na	2.497
A(m)	7.0(5)	0.09 K + 0.48 Na	2.664
A(2)	4.5(5)	0.41 Na	2.596

\*Fixed values are listed as integers and without standard deviations.

TABLE 5. BOND-VALENCE (*vu*) TABLE FOR GEM PARGASITE

	M(1)	M(2)	M(3)	M(4)	A(m)	A(2)	T(1)	T(2)	Σ
O(1)	0.369 <sup>x2↓</sup>	0.327 <sup>x2↓</sup>	0.363 <sup>x4↓</sup>				0.946		2.005
O(2)	0.343 <sup>x2↓</sup>	0.345 <sup>x2↓</sup>		0.273 <sup>x2↓</sup>				0.999	1.960
O(3)	0.315 <sup>x2↓</sup> x2→		0.341 <sup>x2↓</sup>						0.971
O(4)		0.408 <sup>x2↓</sup>		0.328 <sup>x2↓</sup>				1.078	1.814
O(5)				0.167 <sup>x2↓</sup>	0.041 <sup>x2↓</sup>	0.053 <sup>x2↓</sup>	0.871	0.929	
O(6)				0.184 <sup>x2↓</sup>	0.064 <sup>x2↓</sup>	0.016 <sup>x2↓</sup>	0.876	0.885	
O(7)					0.142, 0.121	0.068 <sup>x2↓</sup>	0.896 <sup>x2→</sup>		2.123
Σ	2.054	2.160	2.134	1.904	0.473	0.276	3.589	3.891	

TABLE 6. CHEMICAL FORMULA OF GEM PARGASITE

O24	wt. %	O24	apfu
SiO <sub>2</sub>	47.26	Si	6.56
Al <sub>2</sub> O <sub>3</sub>	12.06	Al	1.44
TiO <sub>2</sub>	0.10	ΣT	8.00
FeO	0.20		
MgO	21.82	Al	0.53
CaO	11.98	Ti	0.01
Na <sub>2</sub> O	4.04	Fe	0.02
K <sub>2</sub> O	0.53	Mg	4.51
F	1.55	ΣC	5.07
H <sub>2</sub> O*	1.43		
O=F	-0.65	Δ	0.07
Total	100.30	Ca	1.78
		Na	0.15
		ΣB	2.00
		Na	0.93
		K	0.09
		ΣA	1.02
		F	0.68
		OH	1.32
		Catsum	16.04

\*Calculated, see text.

rely on mean bond-lengths to assign Al as the sizes of <sup>6</sup>Mg ( $r = 0.72 \text{ \AA}$ ) and <sup>6</sup>Al ( $r = 0.535 \text{ \AA}$ ) are significantly different (Shannon 1976). Hawthorne & Oberti (2007) developed equations relating  $\langle M(1)\text{-O} \rangle$ ,  $\langle M(2)\text{-O} \rangle$ , and  $\langle M(3)\text{-O} \rangle$  distances to constituent cation and anion radii and to other stereochemical aspects of the adjacent sites. Using these equations gives Al site-populations of 0.01, 0.30, and 0.12 *apfu* for  $M(1)$ ,  $M(2)$ , and  $M(3)$ , respectively. These values sum to 0.43 *apfu*, to be compared with 0.53 *apfu* for C-group Al (Table 6). Assigning the site populations to fit the mean bond-lengths and the unit formula equally well gives the values in Table 4. The sum of the bond valences incident at the  $M(3)$  site (Table 5) is 2.13 *vu*, in close accord with the aggregate charge at the  $M(3)$  site (2.14+) calculated from the site populations of Table 4.

#### The $M(4)$ site

There is a slight excess of C-group cations (0.07 *apfu*; Table 6) that would normally be assigned to the  $M(4)$  site. However, in the present case, the resulting site-populations are slightly better if we assume that this slight excess is due to minor uncertainty in the C-group cations. Thus there is no slight excess of A cations in the formula (*cf.* Table 6), and the resulting site-population is in exact accord with the refined site-scattering value (Table 4).

#### The A site

In accord with the work of Hawthorne & Grundy (1972, 1973a, b) and Hawthorne *et al.* (1996c) on local order-disorder in the A cavity in monoclinic amphiboles, we assign Na to the  $A(2)$  site and (Na + K) to the  $A(m)$  site (Table 4) (with the K content taken from the unit formula), in accord with the refined site-scattering values at the  $A(m)$  and  $A(2)$  sites. The aggregate A-site content from the refinement [0.98 (Na + K) *apfu*] (Table 4) agrees closely with that indicated by the unit formula.

#### LONG-RANGE ORDER

Above, we saw that <sup>6</sup>Al is excluded from  $M(1)$  and disordered over  $M(2)$  and  $M(3)$ , a distinctly different arrangement than that assumed in early crystal-structure work, where octahedrally coordinated trivalent cations were assumed to order at the  $M(2)$  site. Infrared spectroscopy by Semet (1973) showed that this is not the case in synthetic amphiboles: the presence of two broad bands centered on 3711 and 3678  $\text{cm}^{-1}$  in synthetic pargasite and magnesio-hastingsite suggests that these bands are due to Al–Mg and Fe<sup>3+</sup>–Mg disorder over the  $M(1)$  and/or  $M(3)$  sites. Welch *et al.* (1994) showed a two-peak <sup>1</sup>H MAS NMR spectrum for pargasite, compatible with disorder of Al over the  $M(2)$  and one or both of the  $M(1,3)$  sites. The disorder of heavier trivalent cations over the  $M(1,3)$  sites was confirmed by Rietveld structure-refinement by Raudsepp *et al.* (1987a, b, 1991), and was also shown to occur in synthetic magnesio-hornblende by Hawthorne *et al.* (2000). Della Ventura *et al.* (1998a) showed that <sup>6</sup>Al is disordered in synthetic pargasite but completely ordered at  $M(2)$  in the Co analogue of pargasite:  $\text{NaCa}_2(\text{Co}^{2+}_4\text{Al})(\text{Si}_6\text{Al}_2)\text{O}_{22}(\text{OH})_2$ , *i.e.*,  $M(1) = M(3) = \text{Co}^{2+}$ .

Detailed crystal-structure work on natural amphiboles by Oberti *et al.* (1995a) showed that <sup>6</sup>Al is partly disordered over the  $M(2)$  and  $M(3)$  sites in Mg-rich pargasite, the degree of disorder increasing with increasing Mg in the structure. In accord with these results, Tait *et al.* (2001) found considerable disorder of Al over  $M(2)$  and  $M(3)$  in a gem-quality Mg-rich pargasite from Baffin Island, and Abdu & Hawthorne (2009) reported intermediate disorder in a more Fe-rich tschermakite. We now see the same sort of disorder in gem pargasite (Table 4, Fig. 2). Some general characteristics are emerging for this type of disorder:

- (1) the degree of disorder is dependent on the size of the larger octahedrally coordinated cation, and decreases significantly in the sequence  $\text{Mg} \rightarrow \text{Co}^{2+} \rightarrow \text{Fe}^{2+}$ ;
- (2) the results of Raudsepp *et al.* (1987a) show that the degree of <sup>6</sup>M<sup>3+</sup> disorder decreases with the radius of the M<sup>3+</sup> cation (from Al to Ga, Cr<sup>3+</sup> to Sc);

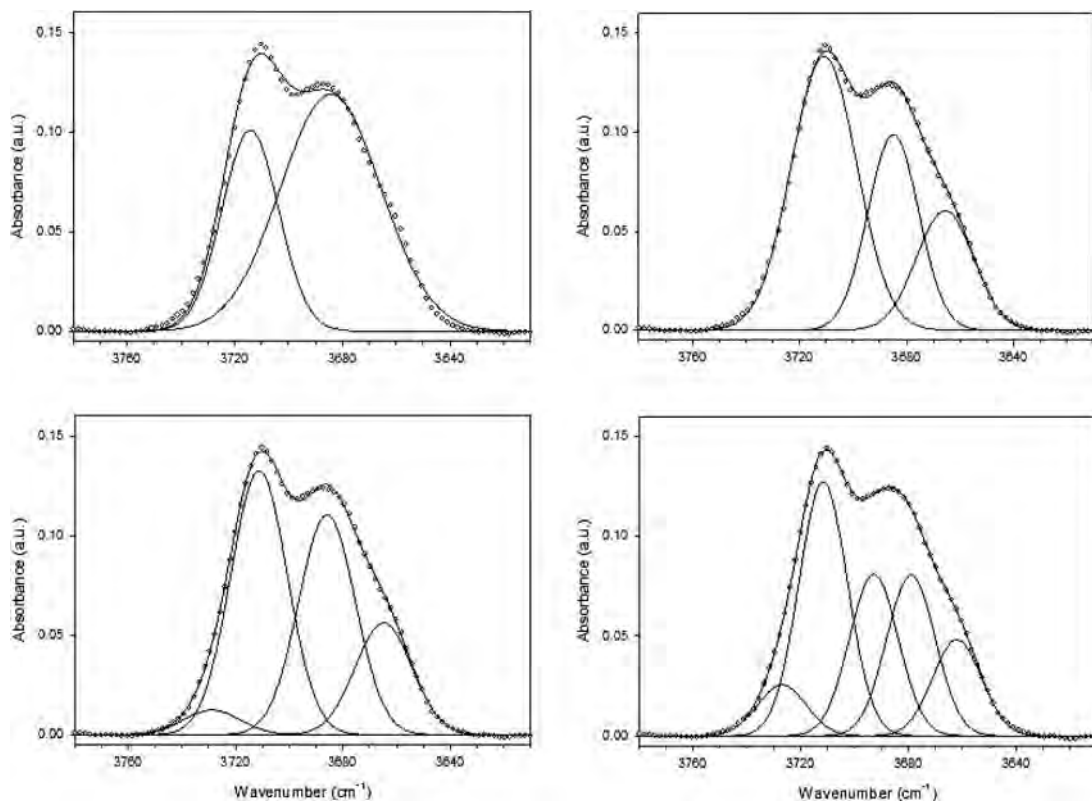


FIG. 2. The infrared spectrum of Myanmar gem pargasite in the principal OH-stretching region fit to two, three, four, and five component peaks.

- (3) the results of Raudsepp *et al.* (1987b) show that there is no  $^{[6]}M^{3+}$  disorder in synthetic Sc-F-pargasite [*i.e.*, where O(3) = F rather than (OH)] or in synthetic Sc-F-eckermannite, synthetic In-F-eckermannite, or synthetic Sc-F-nybøite; Boschmann *et al.* (1994) and Oberti *et al.* (1995b, 1998) showed by single-crystal structure refinement that there is no  $^{[6]}M^{3+}$  disorder in synthetic fluoro-amphiboles; Jenkins & Hawthorne (1995) showed by Rietveld refinement that all  $^{[6]}Ga$  is ordered at  $M(2)$  in  $Ca_2Mg_5Si_8O_{22}F_2-NaCa_2Mg_4Ga_3Si_6O_{22}F_2$  solid-solutions; Gianfagna & Oberti (2001) showed that there is no  $^{[6]}Al$  disorder in fluoro-edenite.
- (4)  $^{[6]}M^{3+}$  disorder occurs in both  $A$ -site-vacant and  $A$ -site-filled amphiboles;
- (5)  $^{[6]}M^{3+}$  disorder occurs in amphiboles where  $B = Ca_2$  and  $B = Na_2$ .

We may make some very interesting conclusions from these five points: (1) the order-disorder seems to

be independent of the charge arrangement in the amphibole and (2) the order-disorder seems to be dependent on sizes of the ions in the amphibole, *i.e.*, the sizes of  $^{[6]}M^{2+}$ ,  $^{[6]}M^{3+}$ , and O(3).

Hawthorne (1978) argued that ordering of heterovalent cations in the  $C2/m$  amphibole structure is dictated by adherence of the structure to Pauling's second rule (the valence-sum rule), and we have been trying to understand the order-disorder relations of divalent and trivalent cations over the  $M(1,2,3)$  sites on this basis. Much of the order of these cations may be explained on this basis, both long range (Oberti *et al.* 2007) and short range (Hawthorne 1997, Hawthorne & Della Ventura 2007, Hawthorne *et al.* 2005, 2006). However, this does not seem to be the case for disorder of Al over  $M(2)$  and  $M(3)$  and its virtual exclusion from  $M(1)$ . The constraints of the valence-sum rule still must hold, but the sizes of the cations and anions (as well as their charges) are also significant, as indicated by the results quoted above. We may examine the effects of variations in sizes of the ions through their influence on the sizes of the  $M(2)$  and  $M(3)$  octahedra:

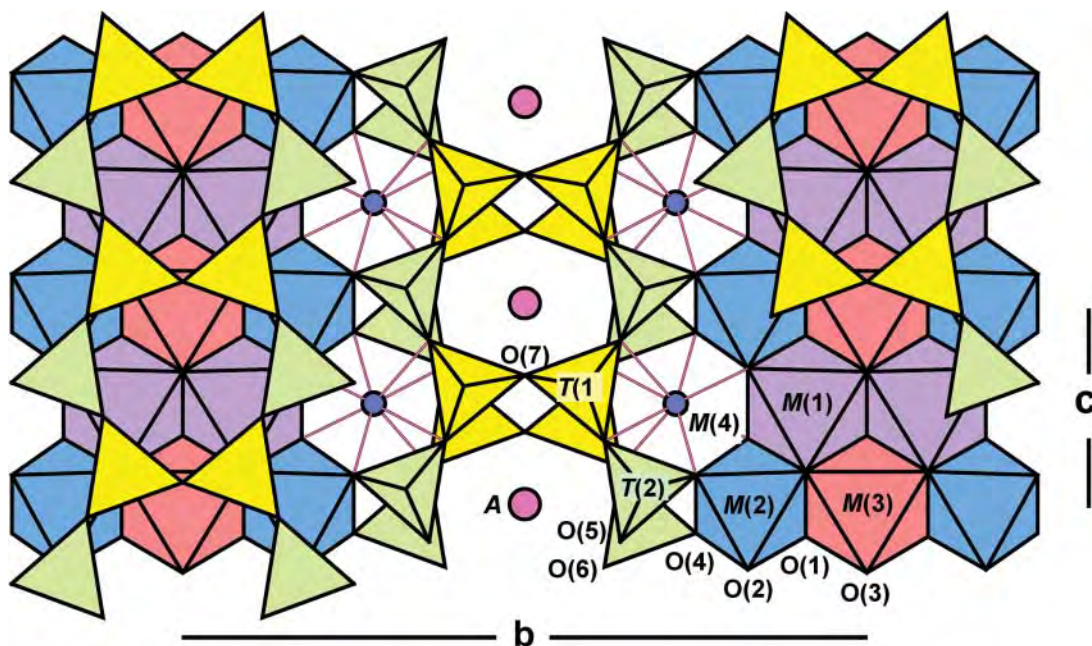


FIG. 3. The  $C2/m$  amphibole structure projected onto (100); polyhedra:  $T(1)$  = yellow,  $T(2)$  = pale green,  $M(1)$  = mauve,  $M(2)$  = blue,  $M(3)$  = pink; sites:  $M(4)$  = blue circle,  $A$  = fuchsia circle.

- (1) Disorder of  $M^{3+}$  between  $M(2)$  and  $M(3)$  tends to reduce the difference in the mean bond-lengths of these two octahedra, and for  $M^{2+} = \text{Mg}$ , disorder decreases as  $M^{3+}$  becomes larger, *i.e.*, as the sizes of the octahedra become more similar.
- (2) Disorder of  $M^{3+}$  between  $M(2)$  and  $M(3)$  vanishes for  $\text{O}(3) = \text{F}$ , *i.e.*,  $\langle M(3)-\text{O} \rangle$  decreases whereas  $\langle M(2)-\text{O} \rangle$  is unaffected, in accord with (1).
- (3) Disorder of  $M^{3+}$  between  $M(2)$  and  $M(3)$  decreases where  $M^{2+}$  becomes larger (*e.g.*, Della Ventura *et al.* 1998a).

Note that (3) acts in the opposite direction to (1) and (2), and hence a simple correlation of disorder with ion size does not occur. The origin of this disorder must await more extensive examination.

#### SHORT-RANGE ORDER

Short-range order involves local clusters of atoms that occur either more or less frequently than predicted by a random distribution. Hawthorne *et al.* (1996a, 1997) showed that short-range order is common in amphiboles, and it is becoming apparent that short-range order can exert major constraints on chemical variations in amphiboles (*e.g.*, Oberti *et al.* 1993)

and other minerals (*e.g.*, Hawthorne *et al.* 1993, Sherriff *et al.* 1991). Extensive work (Hawthorne *et al.* 1997, 2000, Della Ventura *et al.* 1999, 2001, 2003, Robert *et al.* 1999, 2000, Hawthorne & Della Ventura 2007) has shown that both the nearest-neighbor and next-nearest-neighbor cations affect the principal OH-stretching frequency of the locally associated (OH) group, and infrared spectroscopy of the principal OH-stretching region is a sensitive probe of both nearest-neighbor and next-nearest-neighbor short-range arrangements in amphiboles.

#### The configuration symbol and possible arrangements

Hawthorne *et al.* (2005) introduced a configuration symbol which denotes the nearest-neighbor and next-nearest-neighbor cation-sites associated with the  $\text{O}(3)$  site that commonly contains the (OH) group:  $M(1)M(1)M(3)-\text{O}(3)-A:T(1)T(1)-M(2)M(2)M(3)-M(2)M(2)$  (Fig. 4). Various types of ions can locally occupy the sites in the configuration symbol, producing different local arrangements. As these ions are locally associated with (OH) at the  $\text{O}(3)$  site, we may use infrared spectroscopy of the principal (OH)-stretching region as a local probe of short-range cation and anion arrangements at the sites of the configuration symbol.

Della Ventura *et al.* (1999) showed that there are 16 possible local arrangements of Mg, Al, and Si over the local configuration  $M(1)M(1)M(3)-\text{O}(3)-A$ :

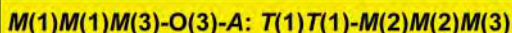
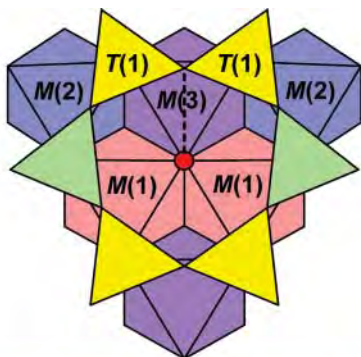


FIG. 4. A fragment of the amphibole structure showing the relevant local association of sites and the corresponding configuration symbol; legend as in Figure 3.

$T(1)T(1)-M(2)M(2)M(3)-M(2)M(2)$  (Table 7) that are reasonably compatible with the local version of the valence-sum rule (Hawthorne 1997). For example, arrangements  $M(1)M(1)M(3)-O(3) = \text{MgAlAl}-(\text{OH})$  and  $\text{AlAlAl}-(\text{OH})$  are prevented by the local version of the valence-sum rule operating at the O(3) site. With regard to the next-nearest-neighbor T(1) sites, the possible occupancies are SiSi and SiAl; the arrangement AlAl is prevented by the local version of the valence-sum rule at O(7) in the absence of Ca at the A site. Thus for the gem pargasite examined here, the possible arrangements of nearest-neighbor cations at  $M(1)M(1)M(3)-A$  are  $\text{MgMgMg}-\text{O}(3)-\text{Na}$  and  $\text{MgMgAl}-\text{O}(3)-\text{Na}$ . With regard to the next-nearest-neighbor M(2) and M(3) sites, the possible occupancies are  $M(1)M(2)M(3) = \text{MgMgMg}$ ,  $\text{MgMgAl}$ ,  $\text{MgAlAl}$ , and  $\text{AlAlAl}$ . These four arrangements may combine with  $M(1)M(1)M(3) = \text{MgMgMg}$ . However, for  $M(1)M(1)M(3) = \text{MgMgAl}$ , only  $M(2)M(2)M(3) = \text{MgMgMg}$  and  $\text{MgMgAl}$  are possible; other arrangements lead to violations of the valence-sum rule at anions coordinated by  $\text{MgAlAl}$  or  $\text{AlAlAl}$ .

Della Ventura *et al.* (1999) also showed that the next-nearest neighbor sites also produce a splitting of the major bands in the spectrum of pargasite. However, this splitting is small with regard to the separation of other bands in the spectrum, and Robert *et al.*

(2000) ignored this splitting in the spectra of pargasite-fluoro-pargasite solid-solutions, successfully treating the split pairs as composite bands; we will adopt the same approach here, and hence we consider only nearest and next-nearest-neighbor effects involving the configuration symbol  $M(1)M(1)M(3)-O(3)-A:T(1)T(1)$  (Fig. 4, Table 7).

#### Constraints of composition

Site populations (Table 4) exert considerable constraints on possible short-range cation arrangements in this structure. Using the site populations of Table 4, we may calculate the relative amounts of the local arrangements for nearest- and next-nearest-neighbor configurations.

**Nearest-neighbor  $M(1)M(1)M(3)$  sites.** The site populations for M(1) and M(3) (Table 4) allow us to calculate the relative amounts of the local arrangements at  $M(1)M(1)M(3)$ :  $\text{MgMgMg}$ :  $\text{MgMgAl} = 0.84:0.16$ .

**Next-nearest-neighbor T(1) site.** Arrangements involving  $T(1)-O(7)-T(1)$  are affected by the amount of  $^{141}\text{Al}$  in the structure. For this gem pargasite,  $T(1)\text{Si} = 2.56$  and  $T(1)\text{Al} = 1.44$  apfu (Table 6). It has been established (see Hawthorne & Oberti 2007 for references) that  $\text{Al}-\text{O}(7)-\text{Al}$  arrangements do not occur unless the O(7) anion is locally associated with Ca at the A site, as in fluoro-cannilloite (Hawthorne *et al.* 1996b). As the gem pargasite examined here has no Ca at the A site (Tables 4 and 6),  $\text{Al}-\text{O}(7)-\text{Al}$  arrangements cannot occur and the composition of this crystal gives the following frequencies of occurrence of these specific arrangements:  $\text{Si}-\text{O}(7)-\text{Al} = 1.44/2 = 0.72$ ;  $\text{Si}-\text{O}(7)-\text{Si} = 0.28$ .

Arrangements involving  $M(1)M(1)M(3) = \text{MgMgMg}$  provide less incident bond-valence for the O(3) anion than arrangements involving  $M(1)M(1)M(3) = \text{MgMgAl}$ . As a result, the O(3)-H bond for  $M(1)M(1)M(3) = \text{MgMgMg}$  is stronger than the O(3)-H bond for  $M(1)M(1)M(3) = \text{MgMgAl}$ . In turn, the H...O(7) hydrogen bond is weaker for  $M(1)M(1)M(3) = \text{MgMgMg}$  than for  $M(1)M(1)M(3) = \text{MgMgAl}$ . This suggests that arrangements involving  $M(1)M(1)M(3) = \text{MgMgMg}$  should be locally associated with the arrangement  $T(1)T(1) = \text{SiSi}$ , and that arrangements involving  $M(1)M(1)M(3) = \text{MgMgAl}$  should be locally associated with the arrangement  $T(1)T(1) = \text{SiAl}$ , as the central O(7) anion requires more bond-valence from the hydrogen bond when linked

TABLE 7. LOCAL ARRANGEMENTS FOR THE CONFIGURATION SYMBOL  $M(1)M(1)M(3)-O(3)-A:T(1)T(1)$  AND FREQUENCIES OF OCCURRENCE OF COMPONENT ARRANGEMENTS

Number	Arrangement	$M(1)M(1)M(3)$	$T(1)T(1)$	Product	Normalized
[1]	$\text{MgMgMg}-\text{OH}-^{\text{A}}\text{Na}:\text{SiSi}$	0.84	0.28	0.235	0.25
[2]	$\text{MgMgMg}-\text{OH}-^{\text{A}}\text{Na}:\text{SiAl}$	0.84	0.72	0.605	0.63
[3]	$\text{MgMgAl}-\text{OH}-^{\text{A}}\text{Na}:\text{SiAl}$	0.16	0.72	0.115	0.12

to SiAl that when linked to SiSi. Accordingly, all  $T(1)T(1) = \text{SiSi}$  arrangements are associated with  $M(1)M(1)M(3) = \text{MgMgMg}$  arrangements in this amphibole.

We may combine the relative frequencies for the various nearest- and next-nearest-neighbor arrangements to get an overall frequency for each of the complete arrangements of Table 7 (with the sum normalized to unity). These values are given in Table 7, and suggest that only arrangements (1), (2), and (4) (Table 8) can give rise to bands of significant intensity in the infrared.

*The nearest-neighbor effect of F.* Each  $M(3)$  site is linked to two (long-range symmetrically equivalent)  $O(3)$  sites, and we may identify three local arrangements involving  $M(3)$  and OH,F: (1) (OH)– $M(3)$ –(OH), (2) (OH)– $M(3)$ –F, and (3) F– $M(3)$ –F. Each of these arrangements is involved in two  $M(1)M(1)M(3)$ – $O(3)$  arrangements, one where the O–H bond points approximately along  $+\mathbf{a}^*$  and the other where the O–H bond points approximately along  $-\mathbf{a}^*$ . Arrangement (1) gives rise to two absorption events in the infrared, arrangement (2) gives rise to one absorption event in the infrared, and arrangement (3) gives rise to no absorption events in the infrared. Thus, irrespective of whether the arrangements of (OH) and F are ordered or disordered relative to the local  $M(3)$  cation, the proportion of absorption events to null-absorption events is equal to the ratio of (OH) to F : 0.66 : 0.34 in this gem pargasite.

Raudsepp *et al.* (1987b) and Oberti *et al.* (1995b) showed that there is no disorder of trivalent cations over  $M(2)$  and  $M(3)$  in amphiboles where  $O(3)$  is occupied by F, a result that means that (at least in the amphiboles examined by them, particularly pargasite) F is strongly to completely locally ordered, *i.e.*, F must be associated with the local arrangement  $M(1)M(1)M(3) = \text{MgMgMg}$  and not with the local arrangement  $\text{MgMgAl}$ . As the arrangement  $M(1)M(1)M(3)$ – $O(3) = \text{MgMgMg}$ –F has no expression in the principal (OH)–stretching region of the infrared, these results indicate that the presence of F preferentially reduces (or even completely suppresses) the expression of the local arrangement  $M(1)M(1)M(3)$ – $O(3) = \text{MgMgMg}$  in the infrared. The data of Della Ventura *et al.* (2014) for fluoro-edenites and fluoro-pargasites from the Franklin marble (USA) are particularly instructive in this regard. The compositions of these five amphiboles have  $6.69 < {}^T\text{Al} < 7.10$  *apfu*, and hence the arrangement  $T(1)T(1) = \text{SiSi}$  must be present in all crystals. However, the F content of these amphiboles is in the range  $1.13 < F < 1.47$  *apfu*, and there is more than enough F to completely “replace” (OH) in the local  $\text{MgMgMg}$ –OH– ${}^A\text{Na}$ :SiSi arrangement, with the result that a band corresponding to  $M(1)M(1)M(3)$ – $O(3)$ –A: $T(1)T(1) = \text{MgMgMg}$ –OH– ${}^A\text{Na}$ :SiSi at  $\sim 3730$   $\text{cm}^{-1}$  does not occur in any of their spectra.

*The next-nearest-neighbor effect of F on the spectrum of gem pargasite*

Robert *et al.* (1999, 2000) showed that amphibole with a filled A site shows two-mode behavior (Chang & Mitra 1968) with regard to the variation in (OH) and F in the structure; gem pargasite, with a filled A site, will show such two-mode behavior. Let  $x$  be the atomic fraction of F:  $x = F/(F + \text{OH})$ , and let  $n_i$  ( $i = 1 \rightarrow 3$ ) be the probability of occurrence of local arrangements OH– ${}^A\text{Na}$ –OH, OH– ${}^A\text{Na}$ –F, and F– ${}^A\text{Na}$ –F such that  $\sum n_i = 1$ . Robert *et al.* (1999) showed that there is no short-range order of the local arrangements in richterite–fluor-richterite (*i.e.*, an A site-filled amphibole) and hence the relative frequencies of these three local arrangements should be as follows:

$$n_1 = (1 - x)^2 / (1 - x + x^2), n_2 = x(1 - x) / (1 - x + x^2), \\ n_3 = x^2 / (1 - x + x^2).$$

For a F content of 0.68 *apfu*,  $x = 0.34$  and  $n_1 = 0.56$ ,  $n_2 = 0.29$ ,  $n_3 = 0.15$ . The arrangement for  $i = 3$  (*i.e.*, F– ${}^A\text{Na}$ –F) is not visible in the infrared, and hence for the composition of the present crystal (F = 0.68 *apfu*), the relative intensities for the normal  $M(1)M(1)M(3)$ –(OH) arrangement (arrangement 1) and the F-shifted  $M(1)M(1)M(3)$ –(OH) arrangement (arrangement 2) are 0.66 and 0.34, respectively. The OH– ${}^A\text{Na}$ –F band will be shifted to lower frequency relative to the OH– ${}^A\text{Na}$ –OH band as in the former arrangement, and Na at the  ${}^A\text{Na}$  site will shift toward F and away from OH to reduce its interaction with H, thereby lowering its vibrational frequency. Moreover, from Robert *et al.* (1999, 2000) we know the approximate relative displacement of the OH– ${}^A\text{Na}$ –OH and OH– ${}^A\text{Na}$ –F bands:  $3730 - 3711 = 19$   $\text{cm}^{-1}$ .

*Assignment of bands in the infrared spectrum of gem pargasite*

The assignment of bands is complicated by the fact that we are unsure of how many there are in the spectrum of Figure 2. Visual inspection of the fits suggests that the two- and three-peak fits are not adequate, and the five-peak fit is somewhat better than the four-peak fit, but this is not surprising, as the fitting process used more parameters. However, the five-peak fit suggests that we have extracted all usable information from the spectrum with this particular fit unless we input more information into the spectrum-fitting process that is external to the spectrum itself, *e.g.*, the number of bands indicated by the chemical composition of the sample. We may use the results of Della Ventura *et al.* (1999) listed in Table 8 to help in the assignment of bands, together with the arrangements of cations and their calculated frequencies given in Table 7. The band frequencies of

TABLE 8. BAND POSITIONS AND INTENSITIES FOR THE FIVE-PEAK FIT TO THE SPECTRUM OF GEM PARGASITE

Band number	Band frequency (cm <sup>-1</sup> )	Normalized absorbance	Assigned band
(1)	3727	0.07	MgMgMg-OH-Na:SiSi
(2)	3712	0.35	MgMgMg-OH-Na:SiAl
(3)	3693	0.22	F-shifted (2)
(4)	3679	0.22	MgMgAl-OH-Na:SiAl
(5)	3662	0.14	F-shifted (4)

Table 8 will not correspond exactly to what we observe here, except for the pargasite band at 3730 cm<sup>-1</sup>, because the peaks may be shifted somewhat from pargasite due to the presence of a significant edenitic component.

The weak band at ~3727 cm<sup>-1</sup> in the four- and five-peak fits corresponds in energy to band (1) of Table 8, and the fact that the band intensity is much less than that expected from the calculations in Table 7 are in accord with our argument that F is associated with the next-nearest-neighbor arrangement  $T(1)T(1) = \text{SiSi}$  (e.g., Della Ventura *et al.* 1998b) which, in turn, will decrease the spectral intensities of all bands associated with local arrangements involving  $T(1)T(1) = \text{SiSi}$ . As noted above, this gem pargasite will show two-mode behavior because of the F content and filled A-site (Table 6), and hence we expect a band due to the F-shifted arrangement (1) at 3727 - 20 = 3707 cm<sup>-1</sup>; this band overlaps with the 3712 cm<sup>-1</sup> band in the fitted spectrum (Table 8), but the latter is the most intense band in the fitted spectrum and must have an intense second component. Note that no other arrangement involving the next-nearest-neighbor arrangement  $T(1)T(1) = \text{SiSi}$  occurs with sufficient frequency to be observed at all.

The most intense band at 3712 cm<sup>-1</sup> is band (2) of Table 8 and arrangement [2] in Table 7: MgMgMg-OH-Na : SiAl. We also expect a band due to the F-shifted arrangement [2] at 3712 - 20 = 3692 cm<sup>-1</sup>, which corresponds to band (3) (Table 8).

The local arrangement involving  $M(1)M(1)M(3) = \text{MgMgAl}$  (arrangement [3], Table 7) is associated with the next-nearest arrangement  $T(1)T(1) = \text{SiAl}$  and corresponds to the band at 3679 cm<sup>-1</sup>. Fluorine avoids this arrangement, and hence there will be no reduction of intensity due to locally associated F. We also expect a band due to the F-shifted arrangement [3] at 3679 - 20 = 3659 cm<sup>-1</sup>, corresponding approximately to band (5) at 3662 cm<sup>-1</sup> in the observed spectrum.

#### Band intensities and arrangement frequencies

We have the following compositional constraints on arrangement proportions (see above discussion):

- (1)  $M(1)M(1)M(3): \text{MgMgMg:MgMgAl} = 0.84:0.16$ .

- (2)  $T(1)T(1): \text{SiSi:SiAl} = 0.28:0.72$ .
- (3) (OH) arrangements (observed in spectrum): F arrangements (not observed in spectrum): 0.66:0.34.
- (4) Proportion of normal bands to F-shifted bands: 0.66:0.34.

We discussed above how F is completely associated with  $M(1)M(1)M(3) = \text{MgMgMg}$  arrangements; thus of the 0.84 MgMgMg arrangements, 0.34 of them are not visible in the infrared due to association with F. Also with regard to these 0.84 MgMgMg arrangements, there are the following arrangements: MgMgMg-SiSi = 0.28, MgMgMg-SiAl = 0.56; above, we suggested that F is preferentially (but not completely) associated with the arrangement MgMgMg-SiSi, and hence the intensity of the band (1) due to the arrangement MgMgMg-(OH)-A-SiSi is reduced in intensity more than that of band (2) due to the arrangement MgMgMg-(OH)-A-SiAl, and inspection of the band intensities in Table 8 shows that this is the case.

The proportion of arrangements MgMgMg: MgMgAl is 0.84:0.16, and the proportion of these bands involving (OH) is 0.84 × 0.66, giving a ratio visible in the infrared of 0.55:0.16 = 0.77:0.23. The corresponding bands in the spectrum of gem pargasite are [(1) + (2) + (3)] and [(4) + (5)], which have an aggregate intensity ratio of 0.64:0.36 (Table 8). The intensity of the lower-energy components [bands (4) and (5)] are therefore enhanced relative to the intensity of the higher-energy components [bands (1), (2), and (3)]. The proportion of normal arrangements to F-shifted arrangements is 0.66:0.34, whereas the analogous bands ratios are 0.35:0.22 = 0.61:0.39 for bands (2) and (3), and 0.22:0.14 = 0.61:0.39 for bands (4) and (5). Again, the intensities of the lower-energy components bands (3) and (5) are therefore enhanced relative to the intensity of the higher-energy components (2) and (4). These relations are in qualitative accord with the relation between transition probability and band frequency (*cf.* Skogby & Rossman 1991, Della Ventura *et al.* 1996, Hawthorne *et al.* 1997).

#### SUMMARY

Although much work remains to be done to fully characterize SRO in amphiboles, some general

patterns of order are emerging. Short-range order is of significance in that it will affect the stability of amphiboles (and other minerals in which it occurs) through its entropy and enthalpy effects. The way in which these effects can be formulated for such a complicated case as the amphibole structure is not yet apparent, but what is clear is that future thermodynamic models need to consider SRO in amphiboles in which heterovalent substitutions are common.

#### ACKNOWLEDGMENTS

We thank Drs. Giancarlo Della Ventura and Mark Welch for their comments and Associate Editor Maria Franca Brigatti for her expert handling of the manuscript. This work was supported by a Canada Research Chair in Crystallography and Mineralogy, Research Tools and Equipment, Discovery and Major Facilities Access Grants to FCH from the Natural Sciences and Engineering Research Council of Canada, and by Canada Foundation for Innovation grants to FCH.

#### REFERENCES

- ABDU, Y. & HAWTHORNE, F.C. (2009) Crystal structure and Mössbauer spectroscopy of tschermakite from the ruby locality at Fiskenaasset, Greenland. *Canadian Mineralogist* **47**, 917–926.
- BOCCHIO, R., UNGARETTI, L., & ROSSI, G. (1978) Crystal chemical study of eclogitic amphiboles from Alpe Arami, Lepontine Alps, Southern Switzerland. *Rendiconti della Società Italiana di Mineralogia e Petrologia* **34**, 453–470.
- BOSCHMANN, K., BURNS, P.C., HAWTHORNE, F.C., RAUDSEPP, M., & TURNOCK, A.C. (1994) A-site disorder in synthetic fluor-edenite, a crystal structure study. *Canadian Mineralogist* **32**, 21–30.
- CHANG, I.F. & MITRA, S.S. (1968) Application of a modified random-element-isodisplacement model to long-wavelength optic phonons of mixed crystals. *Physical Review* **172**, 924–933.
- DELLA VENTURA, G., ROBERT, J.-L., & HAWTHORNE, F.C. (1996) Infrared spectroscopy of synthetic (Ni,Mg,Co)-potassium-richrichterite. In *Mineral Spectroscopy: A Tribute to Roger G. Burns* (M.D. Dyar, C. McCammon, & M.W. Schaefer, eds.). *The Geochemical Society Special Publication* **5**, 55–63.
- DELLA VENTURA, G., ROBERT, J.-L., HAWTHORNE, F.C., RAUDSEPP, M., & WELCH, M.D. (1998a) Contrasting patterns of <sup>61</sup>Al order in synthetic pargasite and Co-substituted pargasite. *Canadian Mineralogist* **36**, 1237–1244.
- DELLA VENTURA, G., ROBERT, J.-L., & HAWTHORNE, F.C. (1998b) Characterization of OH-F short-range order in potassium-fluor-richrichterite by infrared spectroscopy in the OH-stretching region. *Canadian Mineralogist* **36**, 181–185.
- DELLA VENTURA, G., HAWTHORNE, F.C., ROBERT, J.-L., DELBOVE, F., WELCH, M.F., & RAUDSEPP, M. (1999) Short-range order of cations in synthetic amphiboles along the richterite-pargasite join. *European Journal of Mineralogy* **11**, 79–94.
- DELLA VENTURA, G., ROBERT, J.-L., SERGENT, J., HAWTHORNE, F.C., & DELBOVE, F. (2001) Constraints on F vs. OH incorporation in synthetic <sup>61</sup>Al-bearing monoclinic amphiboles. *European Journal of Mineralogy* **13**, 841–847.
- DELLA VENTURA, G., HAWTHORNE, F.C., ROBERT, J.-L., & IEZZI, G. (2003) Synthesis and infrared spectroscopy of amphiboles along the tremolite-pargasite join. *European Journal of Mineralogy* **15**, 341–347.
- DELLA VENTURA, G., OBERTI, R., HAWTHORNE, F.C., & BELLATRECCIA, F. (2007) FTIR spectroscopy of Ti-rich pargasites from Lherz and the detection of O2B at the anionic O3 site in amphiboles. *American Mineralogist* **92**, 1645–1651.
- DELLA VENTURA, G., BELLATRECCIA, F., CÁMARA, F., & OBERTI, R. (2014) Crystal-chemistry and short-range order of fluoro-edenite and fluoro-pargasite: a combined X-ray diffraction and FTIR spectroscopic approach. *Mineralogical Magazine* **78**, 293–310.
- GIANFAGNA, A. & OBERTI, R. (2001) Fluoro-edenite from Biancavilla (Catania, Sicily, Italy): Crystal chemistry of a new amphibole end-member. *American Mineralogist* **86**, 1489–1493.
- GOTTSCHALK, M. & ANDRUT, M. (2003) Crystal chemistry of tremolite-tschermakite solid solutions. *Physics and Chemistry of Minerals* **30**, 108–124.
- HAWTHORNE, F.C. (1978) The crystal chemistry of the amphiboles. IX. Polyvalent cation ordering in amphiboles. *Canadian Mineralogist* **16**, 521–525.
- HAWTHORNE, F.C. (1981) Crystal chemistry of the amphiboles. *Reviews in Mineralogy* **9A**, 1–102.
- HAWTHORNE, F.C. (1983a) The crystal chemistry of the amphiboles. *Canadian Mineralogist* **21**, 173–480.
- HAWTHORNE, F.C. (1983b) Characterization of the average structure of natural and synthetic amphiboles. *Periodico di Mineralogia* **52**, 543–581.
- HAWTHORNE, F.C. (1997) Short-range order in amphiboles: a bond-valence approach. *Canadian Mineralogist* **35**, 201–216.
- HAWTHORNE, F.C. & DELLA VENTURA, G. (2007) Short-range order in amphiboles. *Reviews in Mineralogy and Geochemistry* **67**, 173–222.
- HAWTHORNE, F.C. & GRUNDY, H.D. (1972) Positional disorder in the A-site of clino-amphiboles. *Nature* **235**, 72.

- HAWTHORNE, F.C. & GRUNDY, H.D. (1973a) The crystal chemistry of the amphiboles. I. Refinement of the crystal structure of ferrotschermakite. *Mineralogical Magazine* **39**, 36–48.
- HAWTHORNE, F.C. & GRUNDY, H.D. (1973b) The crystal chemistry of the amphiboles. II. Refinement of the crystal structure of oxykaersutite. *Mineralogical Magazine* **39**, 390–400.
- HAWTHORNE, F.C. & GRUNDY, H.D. (1977) The crystal chemistry of the amphiboles. III. Refinement of the crystal structure of a sub-silicic hastingsite. *Mineralogical Magazine* **41**, 43–50.
- HAWTHORNE, F.C. & OBERTI, R. (2007) Amphiboles: Crystal chemistry. *Reviews in Mineralogy and Geochemistry* **67**, 1–54.
- HAWTHORNE, F.C., UNGARETTI, L., OBERTI, R., CAUCIA, F., & CALLEGARI, A. (1993) The crystal chemistry of staurolite. I. Crystal structure and site-populations. *Canadian Mineralogist* **31**, 551–582.
- HAWTHORNE, F.C., UNGARETTI, L., & OBERTI, R. (1995) Site populations in minerals: terminology and presentation of results of crystal-structure refinement. *Canadian Mineralogist* **33**, 907–911.
- HAWTHORNE, F.C., DELLA VENTURA, G., & ROBERT, J.-L. (1996a) Short-range order of (Na,K) and Al in tremolite: An infrared study. *American Mineralogist* **81**, 782–784.
- HAWTHORNE, F.C., OBERTI, R., UNGARETTI, L., & GRICE, J.D. (1996b) A new hyper-calcic amphibole with Ca at the A site: Fluor-cannilloite from Pargas, Finland. *American Mineralogist* **81**, 995–1002.
- HAWTHORNE, F.C., OBERTI, R., & SARDONE, N. (1996c) Sodium at the A site in clinoamphiboles: the effects of composition on patterns of order. *Canadian Mineralogist* **34**, 577–593.
- HAWTHORNE, F.C., DELLA VENTURA, G., ROBERT, J.-L., WELCH, M.F., RAUDSEPP, M., & JENKINS, D.M. (1997) A Rietveld and infrared study of synthetic amphiboles along the potassium-richterite–tremolite join. *American Mineralogist* **82**, 708–716.
- HAWTHORNE, F.C., WELCH, M.D., DELLA VENTURA, G., LIU, S., ROBERT, J.-L., & JENKINS, D.M. (2000) Short-range order in synthetic aluminous tremolites: An infrared and triple-quantum MAS NMR study. *American Mineralogist* **85**, 1716–1724.
- HAWTHORNE, F.C., DELLA VENTURA, G., OBERTI, R., ROBERT, J.-L., & IEZZI, G. (2005) Short-range order in minerals: amphiboles. *Canadian Mineralogist* **43**, 1895–1920.
- HAWTHORNE, F.C., OBERTI, R., & MARTIN, R.F. (2006) Short-range order in amphiboles from the Bear Lake Diggings, Ontario. *Canadian Mineralogist* **44**, 1171–1179.
- HAWTHORNE, F.C., OBERTI, R., HARLOW, G.E., MARESCH, W., MARTIN, R.F., SCHUMACHER, J.C., & WELCH, M.D. (2012) Nomenclature of the amphibole super-group. *American Mineralogist* **97**, 2031–2048.
- INTERNATIONAL TABLES FOR X-RAY CRYSTALLOGRAPHY (1992) Kluwer Academic Publishers, V.C. Dordrecht, Netherlands.
- JENKINS, D.M. & HAWTHORNE, F.C. (1995) Synthesis and Rietveld refinement of amphiboles along the join  $\text{Ca}_2\text{Mg}_5\text{Si}_8\text{O}_{22}\text{F}_2\text{-NaCa}_2\text{Mg}_4\text{Ga}_3\text{Si}_6\text{O}_{22}\text{F}_2$ . *Canadian Mineralogist* **33**, 13–24.
- JENKINS, D.M., SHERRIFF, B.L., CRAMER, J., & XU, Z. (1997) Al, Si, and Mg occupancies in tetrahedrally and octahedrally coordinated sites in synthetic aluminous tremolite. *American Mineralogist* **82**, 280–290.
- LUPULESCU, M.V., RAKOVAN, J., ROBINSON, G.W., & HUGHES, J.M. (2005) Fluoropargasite, a new member of the calcic amphiboles from Edenville, Orange County, New York. *Canadian Mineralogist* **43**, 1423–1428.
- NAJORKA, J. & GOTTSCHALK, M. (2003) Crystal chemistry of tremolite – tschermakite solid solution. *Physics and Chemistry of Minerals* **30**, 108–124.
- OBERTI, R., UNGARETTI, L., CANNILLO, E., & HAWTHORNE, F.C. (1993) The mechanism of Cl incorporation in amphibole. *American Mineralogist* **78**, 746–752.
- OBERTI, R., HAWTHORNE, F.C., UNGARETTI, L., & CANNILLO, E. (1995a)  $^{16}\text{Al}$  disorder in amphiboles from mantle peridotites. *Canadian Mineralogist* **33**, 867–878.
- OBERTI, R., SARDONE, N., HAWTHORNE, F.C., RAUDSEPP, M., & TURNOCK, A.C. (1995b) Synthesis and crystal-structure refinement of synthetic fluor-pargasite. *Canadian Mineralogist* **33**, 25–31.
- OBERTI, R., HAWTHORNE, F.C., CAMARA, F., & RAUDSEPP, M. (1998) Synthetic fluoro-amphiboles: site preferences of Al, Ga, Sc and inductive effects on mean bond-lengths of octahedra. *Canadian Mineralogist* **36**, 1245–1252.
- OBERTI, R., HAWTHORNE, F.C., CANNILLO, E., & CÁMARA, F. (2007) Long-range order in amphiboles. *Reviews in Mineralogy and Geochemistry* **67**, 125–171.
- PAPIKE, J.J., CAMERON, K.L., & BALDWIN, K. (1969) Crystal chemical characterization of clinoamphiboles based on five new structure refinements. *Mineralogical Society of America Special Paper* **2**, 117–136.
- POUCHOU, J.L. & PICOIR, F. (1985) ‘PAP’  $\phi(\rho Z)$  procedure for improved quantitative microanalysis. In *Microbeam Analysis* (J.T. Armstrong, ed.). San Francisco Press, San Francisco, California, United States (104–106).
- RAUDSEPP, M., TURNOCK, A.C., HAWTHORNE, F.C., SHERRIFF, B.L., & HARTMAN, J.S. (1987a) Characterization of synthetic pargasitic amphiboles ( $\text{NaCa}_2\text{Mg}_4\text{M}^{3+}\text{Si}_6\text{Al}_2\text{O}_{22}(\text{OH},\text{F})_2$ ;  $\text{M}^{3+} = \text{Al, Cr, Ga, Sc, In}$ ) by infrared spectroscopy, Rietveld structure refinement and  $^{27}\text{Al}$ ,  $^{29}\text{Si}$ , and  $^{19}\text{F}$  MAS NMR spectroscopy. *American Mineralogist* **72**, 580–593.

- RAUDSEPP, M., TURNOCK, A.C., & HAWTHORNE, F.C. (1987b) Characterization of cation ordering in synthetic scandium-fluor-eckermannite, indium-fluor-eckermannite and scandium-fluor-nyböite by Rietveld structure refinement. *American Mineralogist* **72**, 959–964.
- RAUDSEPP, M., TURNOCK, A.C., & HAWTHORNE, F.C. (1991) Amphiboles synthesis at low-pressure: what grows and what doesn't. *European Journal of Mineralogy* **3**, 983–1004.
- ROBERT, J.-L., DELLA VENTURA, G., & HAWTHORNE, F.C. (1999) Near-infrared study of short-range disorder of OH and F in monoclinic amphiboles. *American Mineralogist* **84**, 86–91.
- ROBERT, J.-L., DELLA VENTURA, G., WELCH, M.D., & HAWTHORNE, F.C. (2000) The OH-F substitution in synthetic pargasite at 1.5 kbar, 850°C. *American Mineralogist* **85**, 926–931.
- ROBINSON, K., GIBBS, G.V., RIBBE, P.H., & HALL, M.R. (1973) Cation distributions in three hornblendes. *American Journal of Science* **273A**, 522–535.
- SEMET, M.P. (1973) A crystal-chemical study of synthetic magnesiohastingsite. *American Mineralogist* **58**, 480–494.
- SHANNON, R.D. (1976) Revised effective ionic radii and systematic studies of interatomic distances in halides and chalcogenides. *Acta Crystallographica* **A32**, 751–767.
- SHELDRIK, G.M. (2008) A short history of SHELX. *Acta Crystallographica* **A64**, 112–122.
- SHERRIFF, B.L., GRUNDY, H.D., HARTMAN, J.S., HAWTHORNE, F.C., & ČERNÝ, P. (1991) The incorporation of alkalis in beryl, a multinuclear MAS-NMR and crystal structure study. *Canadian Mineralogist* **29**, 271–285.
- SKOGBY, H. & ROSSMAN, G.R. (1991) The intensity of amphibole OH bands in the infrared absorption spectrum. *Physics and Chemistry of Minerals* **18**, 64–68.
- TAIT, K.T., HAWTHORNE, F.C., & DELLA VENTURA, G. (2001) Al-Mg disorder in a gem-quality pargasite from Baffin island, Nunavut, Canada. *Canadian Mineralogist* **39**, 1725–1732.
- WELCH, M.D. & KNIGHT, K.S. (1999) A neutron powder diffraction study of cation ordering in high-temperature synthetic amphiboles. *European Journal of Mineralogy* **11**, 321–331.
- WELCH, M.D., KOŁODZIEJSKI, W., & KLINOWSKI, J. (1994) A multinuclear NMR study of synthetic pargasite. *American Mineralogist* **79**, 261–268.
- WELCH, M.D., LIU, S., & KLINOWSKI, J. (1998) <sup>29</sup>Si MAS NMR systematics of calcic and sodic-calcic amphiboles. *American Mineralogist* **83**, 85–96.

Received December 23, 2014, revised manuscript accepted May 19, 2015.

